HHS Public Access

Author manuscript

J Am Chem Soc. Author manuscript; available in PMC 2022 April 06.

Published in final edited form as:

J Am Chem Soc. 2021 November 24; 143(46): 19257–19261. doi:10.1021/jacs.1c07069.

Proximity-dependent labeling of Cysteines

Sudeshna Sen[1,2], **Nadia Sultana**[1,3], **Scott A. Shaffer**[1,3], **Paul R. Thompson**[*,1,2]

[1]Department of Biochemistry and Molecular Pharmacology, University of Massachusetts Medical School, 364 Plantation Street, Worcester, Massachusetts 01605, United States.

[2]Program in Chemical Biology, University of Massachusetts Medical School, 364 Plantation Street, Worcester, Massachusetts 01605, United States.

[3]Mass Spectrometry Facility, University of Massachusetts Medical School, Shrewsbury, Massachusetts 01545, United States.

Abstract

Mapping protein-protein interactions is crucial for understanding various signaling pathways in living cells and developing new techniques for this purpose has attracted significant interest. Classic methods (e.g., the yeast two-hybrid) have been supplanted by more sophisticated chemical approaches that label proximal proteins (e.g., BioID, APEX). Herein, we describe a proximity-based approach that uniquely labels cysteines. Our approach exploits the NNMT-catalyzed methylation of an alkyne-substituted 4-chloropyridine (**SS6**). Upon methylation of the pyridinium nitrogen, this latent electrophile diffuses out of the active site and labels proximal proteins on short time-scales (≤ 5 min). We validated this approach by identifying known (and novel) interacting partners of protein arginine deiminase 2 (PAD2) and pyruvate dehydrogenase kinase 1 (PDK1). To our knowledge, this technology uniquely exploits a suicide substrate to label proximal cysteines in live cells.

Graphical Abstract

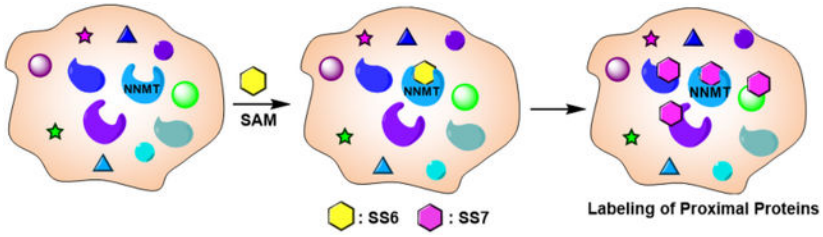

[*]**Corresponding Author:** Department of Biochemistry and Molecular Pharmacology, University of Massachusetts Medical School, LRB 826, 364 Plantation Street, Worcester MA 01605. Tel.: 508-856-8492. Fax: 508-856-6215. paul.thompson@umassmed.edu.

Author Contributions

The manuscript was written through contributions of all authors. / All authors have given approval to the final version of the manuscript.

Supporting information. Complete methods, Figures S1–S26, Tables S1–S2, supporting references, raw ratios and supporting data for proteomics experiments (Supplementary data 1). This material is available free of charge via the Internet at http://pubs.acs.org.

The authors declare no competing financial interests.

Protein-protein interactions play pivotal roles in numerous cellular processes and detecting transient binding interactions without perturbing the cellular microenvironment remains a major challenge.[1] Historically, yeast two-hybrid strategies and affinity-purification mass spectrometry (AP-MS) approaches have been used to identify cellular interactomes.[2, 3] However, the difficulty of purifying intact organelles restricts their utility. Proximity-based approaches wherein the protein-of-interest is fused to a promiscuous enzyme, including a biotin ligase (for BioID and TurboID) and engineered ascorbate peroxidase (for APEX), have come to the foreground.[4–8] Despite the success of these approaches, there are key limitations that can bias efficient labeling. For example, H_2O_2 used in APEX labeling is toxic for living cells and can affect redox sensitive pathways. Furthermore, ubiquitous expression of TurboID induces cellular toxicity by sequestering endogenous biotin. Herein, we report a proximity-based strategy to identify interacting proteins with fast kinetics and high spatial control without inducing significant cellular toxicity (Figure 1). This approach exploits an alkyne-substituted 4-chloropyridine (**SS6**) that is a suicide substrate of Nicotinamide N-methyl transferase (NNMT).[9] Methylation of the pyridinium nitrogen generates the highly electrophilic N-methyl-4-chloropyridine (**SS7**) which diffuses out of the active site and reacts with cysteines on proximal proteins.[9, 10] The labeled proteins are then linked to biotin-azide via copper-catalyzed azide-alkyne cycloaddition (CuAAC) chemistry, affinity-captured on the streptavidin beads, and identified by tandem mass spectrometry. To demonstrate the utility of this technique, we fused NNMT, independently, to protein arginine deiminase 2 (PAD2) and pyruvate dehydrogenase kinase 1 (PDK1). These enzymes localize to specific organelles in cells. Using this technique, we identified the cellular interactome of PAD2 and PDK1. Notably, the labeling kinetics are extremely fast (≤ 5 minutes) and highly organelle specific.

Nicotinamide N-methytransferase (NNMT) catalyzes the S-adenosyl-L-methionine (SAM)-dependent methylation of nicotinamide (NAM) to form N-methylnicotinamide (Me-NAM) (Figure 1A).[11, 12] This enzyme detoxifies xenobiotics[13] and regulates NAD^+ biosynthesis.[14, 15] Previously, we reported a novel suicide-inhibition based labeling strategy, SIBLing that utilizes 4-chloropyridine moieties as NNMT substrates to generate the corresponding N-methylated products which in turn inhibit the enzyme by covalently modifying an allosteric cysteine.[9] We also developed a suicide probe, an alkyne-substituted 4-chloropyridine (**SS6**, Figure 1B) that can be conjugated with a reporter tag via CuAAC after enzyme inactivation. Notably, **SS6** labels NNMT both *in vitro*, in cells overexpressing NNMT (HEKNNMT, Figure S1A), and in cells that endogenously express NNMT at high levels (e.g., SKOV3 cells, Figure S1B). In addition to NNMT, **SS6** labels multiple other proteins (Figure S1). This modification is NNMT-dependent because labeling is muted in cells expressing either low levels of NNMT or a catalytically inactive mutant of NNMT (Y20A) but is increased by adding recombinant NNMT to cell lysates (Figure S1C, S2). This effect relates to the fact that N-methylation is ~200 times faster than enzyme inactivation.[9] Consequently, the N-methylated product can diffuse away from the active site and covalently modify accessible cysteines on proximal proteins (Figure 1C, D).

To validate the utility of this approach, we first sought to identify proteins that interact with protein arginine deiminase 2 (PAD2), a member of the PAD family of enzymes that

mediate the post-translational conversion of arginine to citrulline.[16, 17] We chose to focus on PAD2 because this enzyme plays important roles in inflammatory diseases and gene transcription.[18, 19] Thus, information on interacting proteins could be broadly useful to define pathways in which this enzyme plays a role. Additionally, we previously applied BioID2 to identify potential PAD2 interacting proteins, thereby providing a dataset to cross validate our findings.[20]

For these studies, we first fused NNMT to the N- and C-terminus of full length human PAD2. In each case, the fusion partners were separated by a GGGGS linker (Figure 2A). After stably expressing the fusion proteins in HEK293T cells, we monitored the activity of both fusion proteins. In presence of calcium, wild-type PAD2 translocates into the nucleus and citrullinates histone H3 and activates transcription.[16, 20] Consistent with prior work, PAD2 and PAD2-NNMT (NNMT fused to C-terminus of PAD2) induce robust citrullination of histone H3 (Figure 2B).

By contrast, H3 is not citrullinated in HEK293T cells which do not express a PAD. Similar results were obtained for the NNMT-PAD2 construct (Figure S3A). To determine whether PAD2 impacted NNMT activity, we measure the rates of quinoline methylation;1-methyl-quinoline is fluorescent.[21] Under these conditions, we only observed a minor decrease in NNMT activity (Figure 2C). Next, we evaluated the subcellular localization of the fusion proteins; PAD2 is normally cytosolic with a fraction of the enzyme translocating into the nucleus upon calcium simulation.[20] For these studies, we generated nuclear and cytosolic fractions for cells expressing PAD2 or PAD2-NNMT. NNMT is retained in the cytosol but when fused to PAD2, the PAD2-NNMT fusion protein translocates into the nucleus just like wild-type PAD2 (Figure 2D). Similar results were obtained for the NNMT-PAD2 construct (Figure S3B). Next, we treated the cells with **SS6** and SAM followed by CuAAC to couple the alkyne to TAMRA-N_3 or Biotin-N_3. Measurement of in-gel fluorescence identified protein labeling in HEK293T cells overexpressing the fusion proteins, regardless of the presence of calcium (Figures 2E–F, S4). Notably, near maximal labeling was achieved after just 5 min of labeling with **SS6** (Figure S5A). Importantly, **SS6** did not induce any significant cellular toxicity to HEKNNMT cells (Figure S5B).

We then identified PAD2 interacting partners by LC-MS/MS analysis. Briefly, cells were treated with **SS6** for 5 min and the labeled proteome was “clicked” to Biotin-N_3. Biotinylated proteins were then selectively captured on streptavidin-agarose beads followed by an on-bead digestion with trypsin. Because the fusion proteins remain in the cytosol in absence of calcium, we compared the proteins enriched from HEKPAD2-NNMT (or HEKNNMT-PAD2 cells) to HEKNNMT cells. However, since calcium triggers the translocation of PAD2 into the nucleus, we could not use HEKNNMT cells as a control because NNMT is a cytosolic enzyme. Therefore, we generated an NNMT-NLS construct, which fuses wild-type NNMT to a C-terminal nuclear localization signal (Figures S6A). As expected, the NNMT-NLS fusion protein is constitutively present in both the cytosol and nucleus (Figure S6B, S7) and serves as the ideal control to map PAD2 interacting partners in the nucleus.

The tryptic digests were reductively dimethylated (ReDiMe) with heavy (PAD2-NNMT), light (NNMT-PAD2) and medium (NNMT or NNMT-NLS) formaldehyde and sodium cyanoborohydride (for light and medium) or sodium cyanoborodeuteride (for heavy samples). Subsequent proteomic analysis afforded the enrichment ratio of the proteins that are covalently modified by **SS**7 (Figure 3A–B, S8A–B). We applied a conservative enrichment cutoff with log2 fold-change > 0 and a T-test corrected P-value <0.05 from three replicates to identify proteins that were significantly enriched in both datasets. A total of 288 proteins were detected in the PAD2-NNMT dataset. Of these, 140 proteins showed a log2 fold change > 0 in the absence of calcium. In the presence of calcium, 155 proteins were enriched (Figure 3A–B). Comparison of both the datasets identified 87 common proteins (Figure S9A). NNMT-PAD2 cells also showed a similar profile (Figure S5, S9B). A comparison of the PAD2-NNMT and NNMT-PAD2 datasets identified 129 common proteins in the presence of calcium (Figure S9C) and 121 in absence of calcium (Figure S9D).

PAD2 was highly enriched in all datasets confirming the proximal labeling and enrichment of the fusion proteins. In addition, many of the enriched proteins were previously reported as PAD2 interacting proteins.[20] For example, BioID2 identified RAN and ANXA5 as PAD2 interacting proteins where RAN modulates the nuclear localization of PAD2 and ANXA5 stabilizes PAD2 in the cytoplasm in the absence of calcium.[20] XRCC5 and XRCC6 were also confirmed to interact with PAD2 in presence of calcium suggesting the possible involvement of PAD2 in DNA repair pathways. This interaction was confirmed via coimmunoprecipitation experiments (Figure S10). Other enriched proteins include substrates (e.g., Histone H3, Heat shock proteins, and Vimentin) that are citrullinated by PAD2 and PAD4.[16, 22–24]

Based on Gene Ontology (GO) enrichment analyses, most of the proteins enriched in the absence of calcium were cytosolic (Figure 3C, S11A). By contrast, there is a shift to nuclear proteins when cells are stimulated with calcium (Figure 3D, S11B). These results are consistent with the known cellular localization of PAD2; calcium triggers the movement of PAD2 from the cytosol into the nucleus.[20] While 52 proteins were found to be common to both BioID2 and SIBLing datasets in presence of calcium (Figure 3E), only 34 common proteins were identified in the absence of calcium (Figure S12). The difference in the number of enriched proteins between SIBLIng and BioID most likely relates to the different reactivity profiles of cysteine and lysine, respectively, as well as the different labeling times (hours with BioID versus minutes with SIBLing). Comparison of SIBLing and BioID2 datasets with known PAD2 substrates identified 37 proteins common to all datasets (Figure 3E, Supplementary Data 1). Overall, these results demonstrate the power and versatility of our approach with labeling times of just 5 min compared to the 12–18 h required for early iterations of BioID.

Having identified known PAD2 interacting proteins and demonstrating that we can monitor the translocation of PAD2 into the nucleus, we next sought to gain further insights into the spatial selectivity of this approach. To that end, we fused NNMT to the gene encoding pyruvate dehydrogenase kinase 1 (PDK1); PDK1 is a mitochondrial enzyme that regulates the activity of pyruvate dehydrogenase.[25, 26] Since the N-terminus of PDK1 is necessary for its mitochondrial localization, NNMT was fused to the C-terminus of full length,

human PDK1 (Figure 4A). After stably expressing the fusion protein in HEK293T cells, we confirmed its mitochondrial localization by generating cytosolic and mitochondrial fractions as well as fluorescence imaging (Figure 4B, S13). Next, we monitored whether this fusion impacted NNMT activity.

Like the PAD2-NNMT fusion proteins, we only observed a minor decrease in NNMT activity in PDK1-NNMT cells (Figure 4C). Furthermore, **SS6** dose dependently labeled cellular proteins in PDK1-NNMT cells. (Figure 4D). To confirm the selective labeling of mitochondrial proteins, we generated mitochondrial and cytosolic fractions of the probe treated cells. Significantly more labeling was observed in the mitochondrial fraction than the cytosolic fraction (Figure S14).

Next, we mapped PDK1 interacting proteins by proteomic analyses. A total of 834 proteins were detected in this dataset. Of these, 477 proteins showed a log2 fold change > 0 (Figure 4E). PDK1 and its substrate pyruvate dehydrogenase were detected amongst the enriched proteins (Figure 4E, S15A). Consistent with the mitochondrial localization of the PDK1-NNMT fusion protein, most enriched proteins were mitochondrial (Figure 4F, S15A). Biological process analysis specifically characterized mitochondria related processes including cellular metabolic processes and oxidation-reduction processes (Figure S15B). These results clearly demonstrate the organelle specific labeling of proximal proteins by **SS6**. Although we observe a lower percentage of mitochondrial proteins relative to the APEX mitochondrial profiling,[27] a key advantage is our ability to selectively label cysteines in cells.

Finally, to confirm cysteine labeling, HEKNNMT cells were treated with **SS6** and SAM for 5 min and the labeled proteome was “clicked” to a photo-cleavable biotin tag. Biotinylated proteins were selectively captured on streptavidin-agarose beads followed by an on-bead digestion with trypsin. The probe-modified peptides were then eluted by irradiating the beads with 365 nm light for 30 min (Figure S16). Subsequent proteomic analyses identified 97 proteins containing one or more peptides modified with SS6 at a cysteine. Manual inspection of a subset of these fragmentation spectra confirmed the presence of diagnostic fragment peaks for the modified (Figures S17–26 and Table S2).

In conclusion, we have developed a novel proximity-based protein labeling technique which exploits an alkyne-substituted 4-chloropyridine, a suicide substrate of NNMT. Upon N-methylation, the highly reactive N-methylated product diffuses out from the active site and reacts with the cysteine residues on proximal proteins. Using this technology, we demonstrated proteome-wide proximity profiling for the enzymes PAD2 and PDK1 in live cells. These studies identified both known and novel interacting proteins of PAD2 and PDK1, and the labeling was highly organelle specific. The major advantage of SIBLing over other available protein labeling techniques is its fast kinetics and catalytic production of the tagging element; 10 μM of **SS6** enabled efficient labeling in just 5 minutes. Future efforts are focused on developing modified labeling methods using *in cellular* click chemistry to precisely define the diffusion radius of **SS7**. We also envision the future use of this technique to identify reactive cysteines in cellular proteomes.

Supplementary Material

Refer to Web version on PubMed Central for supplementary material.

ACKNOWLEDGEMENTS

S.S. and P.R.T. thank Prof. Eranthie Weerapana (Boston College) for her valuable suggestions. S.S. thanks Dr. Shreya Roy Chowdhury (UMass Chan Medical School) for her help in recording the fluorescence microscopy images.

Funding Sources

This work was supported in part by NIH grants R35 GM118112 (P.R.T.).

ABBREVIATIONS

SIBLing	Suicide Inhibition Based Protein Labeling
PAD	Protein Arginine Deiminase
NLS	Nuclear Localization Signal
ReDiMe	Reductive DiMethylation

REFERENCES

1. Scott JD; Pawson T, Cell signaling in space and time: where proteins come together and when they’re apart. Science 2009, 326 (5957), 1220–4. [PubMed: 19965465]
2. Parrish JR; Gulyas KD; Finley RL, Yeast two-hybrid contributions to interactome mapping. Curr. Opin. Biotechnol 2006, 17 (4), 387–393. [PubMed: 16806892]
3. Young KH, Yeast Two-hybrid: So Many Interactions, (in) So Little Time. Biol. Reprod 1998, 58 (2), 302–311. [PubMed: 9475380]
4. Branon TC; Bosch JA; Sanchez AD; Udeshi ND; Svinkina T; Carr SA; Feldman JL; Perrimon N; Ting AY, Efficient proximity labeling in living cells and organisms with TurboID. Nat. Biotechnol 2018, 36 (9), 880–887. [PubMed: 30125270]
5. Chen C-L; Perrimon N, Proximity-dependent labeling methods for proteomic profiling in living cells. Wiley Interdiscip. Rev. Dev. Biol 2017, 6 (4), e272.
6. Lam SS; Martell JD; Kamer KJ; Deerinck TJ; Ellisman MH; Mootha VK; Ting AY, Directed evolution of APEX2 for electron microscopy and proximity labeling. Nat. Methods 2015, 12 (1), 51–54. [PubMed: 25419960]
7. Roux KJ, Marked by association: techniques for proximity-dependent labeling of proteins in eukaryotic cells. Cell. Mol. Life. Sci 2013, 70 (19), 3657–64. [PubMed: 23420482]
8. Roux KJ; Kim DI; Raida M; Burke B, A promiscuous biotin ligase fusion protein identifies proximal and interacting proteins in mammalian cells. J Cell Biol 2012, 196 (6), 801–10. [PubMed: 22412018]
9. Sen S; Mondal S; Zheng L; Salinger AJ; Fast W; Weerapana E; Thompson PR, Development of a Suicide Inhibition-Based Protein Labeling Strategy for Nicotinamide N-Methyltransferase. ACS Chem. Biol 2019, 14 (4), 613–618. [PubMed: 30933557]
10. Schardon CL; Tuley A; Er JAV; Swartzel JC; Fast W, Selective Covalent Protein Modification by 4-Halopyridines through Catalysis. ChemBioChem 2017, 18 (15), 1551–1556. [PubMed: 28470883]
11. Aksoy S; Szumlanski CL; Weinshilboum RM, Human liver nicotinamide N-methyltransferase. cDNA cloning, expression, and biochemical characterization. J. Biol. Chem 1994, 269 (20), 14835–14840. [PubMed: 8182091]

12. Rini J; Szumlanski C; Guerciolini R; Weinshilboum RM, Human liver nicotinamide N-methyltransferase: Ion-pairing radiochemical assay, biochemical properties and individual variation. Clin. Chim. Acta 1990, 186 (3), 359–374. [PubMed: 2311261]
13. Thomas MG; Sartini D; Emanuelli M; van Haren MJ; Martin NI; Mountford DM; Barlow DJ; Klamt F; Ramsden DB; Reza M; Parsons RB, Nicotinamide N-methyltransferase catalyses the N-methylation of the endogenous β-carboline norharman: evidence for a novel detoxification pathway. Biochem. J 2016, 473 (19), 3253–3267. [PubMed: 27389312]
14. Kraus D; Yang Q; Kong D; Banks AS; Zhang L; Rodgers JT; Pirinen E; Pulinilkunnil TC; Gong F; Wang Y.-c.; Cen Y; Sauve AA; Asara JM; Peroni OD; Monia BP; Bhanot S; Alhonen L; Puigserver P; Kahn BB, Nicotinamide N-methyltransferase knockdown protects against diet-induced obesity. Nature 2014, 508 (7495), 258–262. [PubMed: 24717514]
15. Riederer M; Erwa W; Zimmermann R; Frank S; Zechner R, Adipose tissue as a source of nicotinamide N-methyltransferase and homocysteine. Atherosclerosis 2009, 204 (2), 412–417. [PubMed: 18996527]
16. Fuhrmann J; Clancy KW; Thompson PR, Chemical Biology of Protein Arginine Modifications in Epigenetic Regulation. Chem. Rev 2015, 115 (11), 5413–5461. [PubMed: 25970731]
17. Mondal S; Thompson PR, Protein Arginine Deiminases (PADs): Biochemistry and Chemical Biology of Protein Citrullination. Acc. Chem. Res 2019, 52 (3), 818–832. [PubMed: 30844238]
18. Jones JE; Causey CP; Knuckley B; Slack-Noyes JL; Thompson PR, Protein arginine deiminase 4 (PAD4): Current understanding and future therapeutic potential. Curr. Opin. Drug. Discov. Devel 2009, 12 (5), 616–627.
19. Witalison EE; Thompson PR; Hofseth LJ, Protein Arginine Deiminases and Associated Citrullination: Physiological Functions and Diseases Associated with Dysregulation. Curr. Drug Targets 2015, 16 (7), 700–710. [PubMed: 25642720]
20. Zheng L; Nagar M; Maurais AJ; Slade DJ; Parelkar SS; Coonrod SA; Weerapana E; Thompson PR, Calcium Regulates the Nuclear Localization of Protein Arginine Deiminase 2. Biochemistry 2019, 58 (27), 3042–3056. [PubMed: 31243954]
21. Neelakantan H; Vance V; Wang H-YL; McHardy SF; Watowich SJ, Noncoupled Fluorescent Assay for Direct Real-Time Monitoring of Nicotinamide N-Methyltransferase Activity. Biochemistry 2017, 56 (6), 824–832. [PubMed: 28121423]
22. Bodnár N; Szekanecz Z; Prohászka Z; Kemény-Beke Á; Némethné-Gyurcsik Z; Gulyás K; Lakos G; Sipka S; Szántó S, Anti-mutated citrullinated vimentin (anti-MCV) and anti-65kDa heat shock protein (anti-hsp65): New biomarkers in ankylosing spondylitis. Joint Bone Spine 2012, 79 (1), 63–66. [PubMed: 21683641]
23. Lu M-C; Yu C-L; Yu H-C; Huang H-B; Koo M; Lai N-S, Anti-citrullinated protein antibodies promote apoptosis of mature human Saos-2 osteoblasts via cell-surface binding to citrullinated heat shock protein 60. Immunobiology 2016, 221 (1), 76–83. [PubMed: 26275591]
24. Travers TS; Harlow L; Rosas IO; Gochuico BR; Mikuls TR; Bhattacharya SK; Camacho CJ; Ascherman DP, Extensive Citrullination Promotes Immunogenicity of HSP90 through Protein Unfolding and Exposure of Cryptic Epitopes. J. Immunol 2016, 197 (5), 1926. [PubMed: 27448590]
25. Bonnet S; Archer SL; Allalunis-Turner J; Haromy A; Beaulieu C; Thompson R; Lee CT; Lopaschuk GD; Puttagunta L; Bonnet S; Harry G; Hashimoto K; Porter CJ; Andrade MA; Thebaud B; Michelakis ED, A Mitochondria-K+Channel Axis Is Suppressed in Cancer and Its Normalization Promotes Apoptosis and Inhibits Cancer Growth. Cancer Cell 2007, 11 (1), 37–51. [PubMed: 17222789]
26. Yeaman SJ; Hutcheson ET; Roche TE; Pettit FH; Brown JR; Reed LJ; Watson DC; Dixon GH, Sites of phosphorylation on pyruvate dehydrogenase from bovine kidney and heart. Biochemistry 1978, 17 (12), 2364–2370. [PubMed: 678513]
27. Rhee HW; Zou P; Udeshi ND; Martell JD; Mootha VK; Carr SA; Ting AY, Proteomic mapping of mitochondria in living cells via spatially restricted enzymatic tagging. Science 2013, 339 (6125), 1328–1331. [PubMed: 23371551]

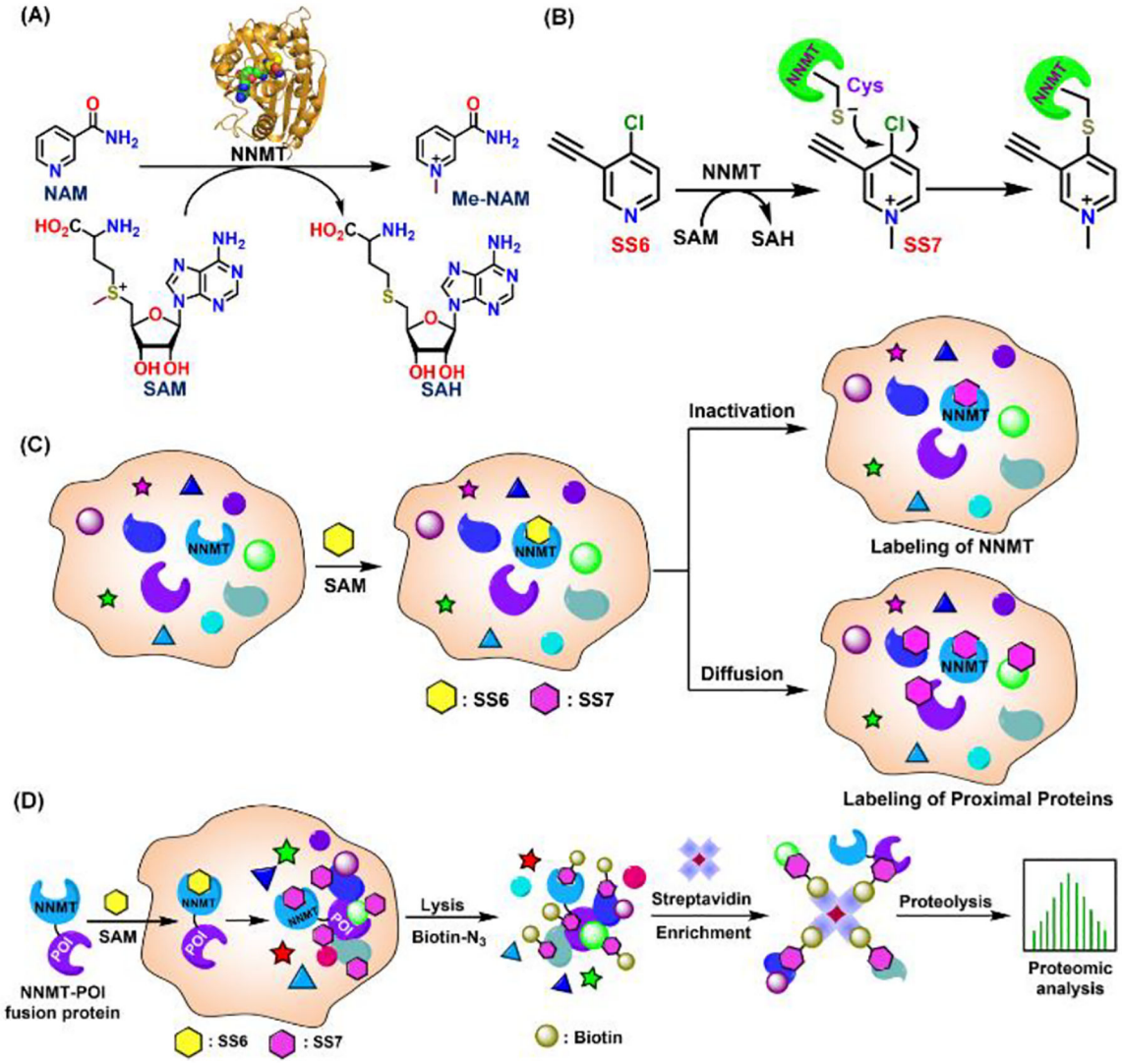

Figure 1.

(A) NNMT reaction. (B) Inactivation of NNMT by **SS6**. (C) Proposed mechanism of NNMT labeling by **SS6**. (D) Schematic representation of SIBLing, a suicide inhibition based proximity protein labeling technique.

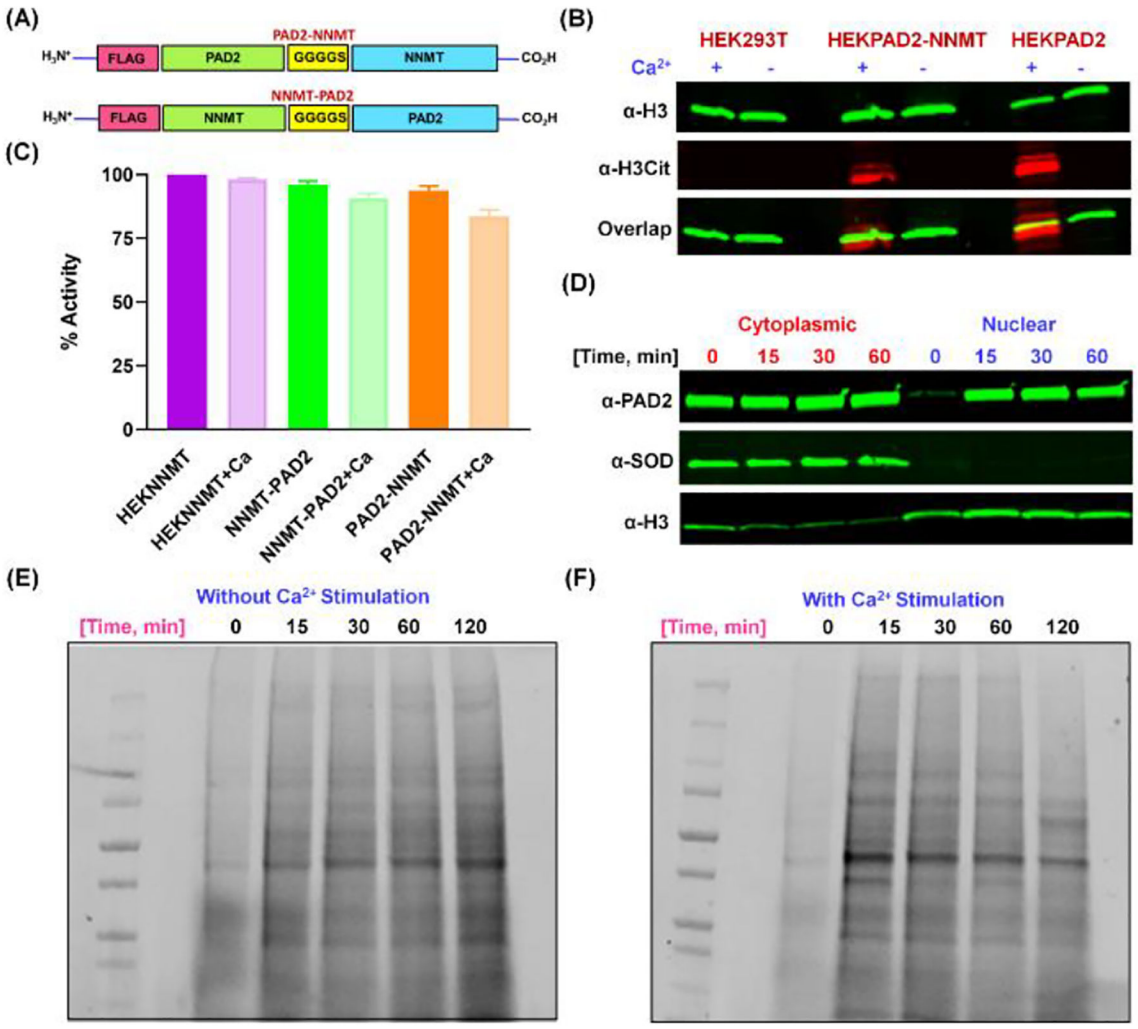

Figure 2.

(A) Constructs encoding the PAD2-NNMT and NNMT-PAD2 fusion proteins. (B) A Histone H3-citrullination assay comparing the relative activity of PAD2-NNMT to WT-PAD2. Citrullinated H3 (H3Cit) and H3 are shown in red and green, respectively. (C) NNMT activity of the fusion proteins was assayed by measuring quinoline methylation (see methods). This experiment was performed in duplicate and the associated errors are SEM. (D) Nuclear/cytosol fractionation of HEKPAD2-NNMT cells. SOD and Histone H3 were cytoplasmic and nuclear controls, respectively. (E) Time-dependent labeling of HEKPAD2-NNMT cells by **SS6**. (F) Time-dependent labeling of calcium stimulated HEKPAD2-NNMT cells by **SS6**. All experiments were performed in triplicate (n = 3).

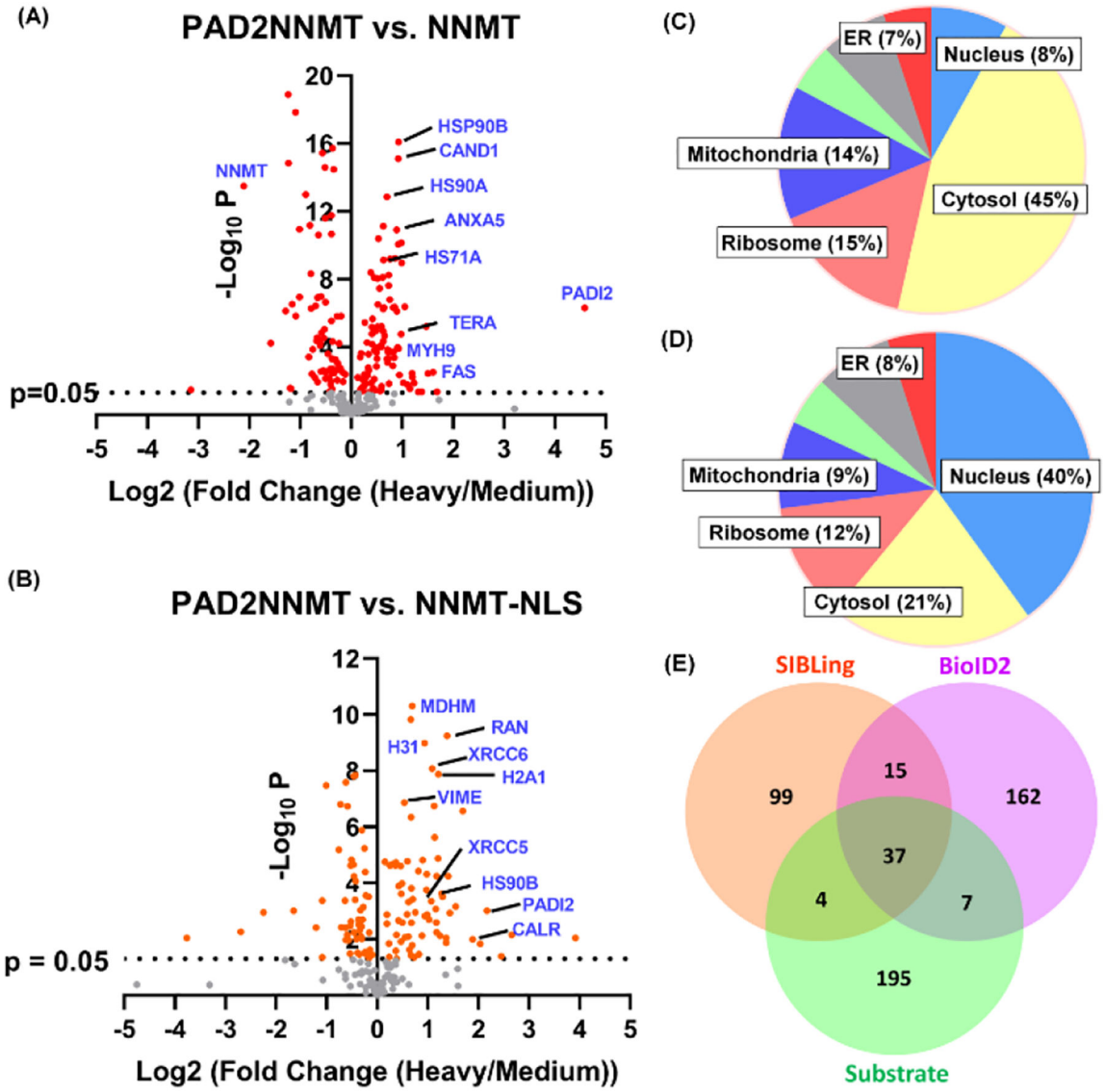

Figure 3.

PAD2 interacting proteins. Volcano Plots showing proteins that are enriched in probe treated HEK-PAD2-NNMT cells (Heavy) compared to HEK-NNMT cells without (A) and with (B) calcium treatment. All experiments were performed in triplicate (n = 3). (C) Gene ontology enrichment analysis (cellular component) of the 140 proteins that are enriched in samples without calcium treatment and (D) the 155 enriched proteins in the calcium treated sample. (E) Venn diagram comparing the number of proteins enriched in the SIBLing and BioID2 dataset to known substrates of PAD2.

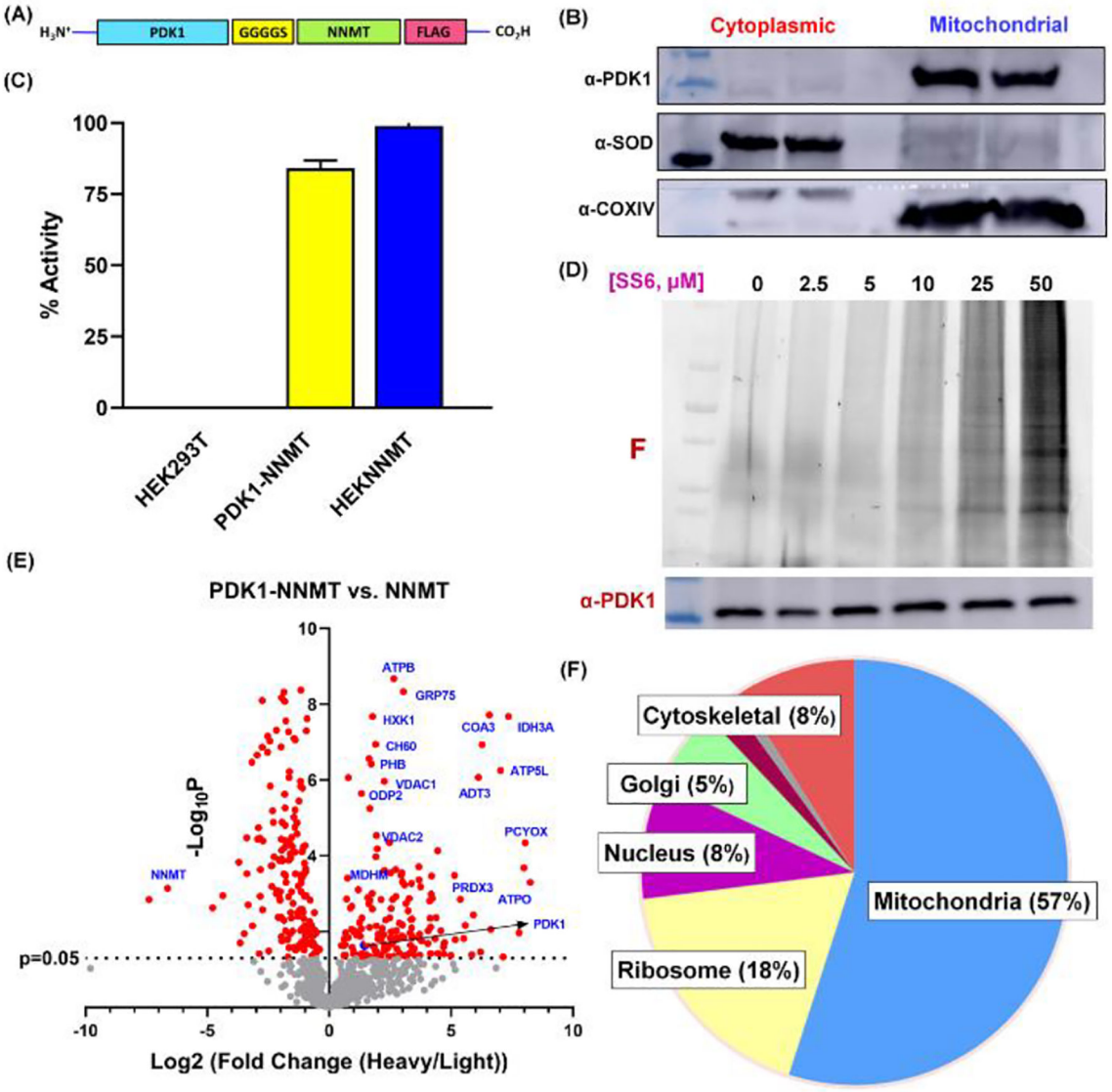

Figure 4.

(A) Genetic fusion of NNMT to PDK1 (PDK1-NNMT). (B) Mitochondrial localization of the PDK1-NNMT fusion protein. SOD and COXIV are cytoplasmic and mitochondrial controls. (C) PDK1-NNMT has comparable activity to WT-NNMT. (D) Concentration-dependent labeling of HEKPDK1-NNMT cells by **SS6** and SAM. (E) Volcano Plots showing proteins that are enriched in probe treated HEKPDK1-NNMT cells (Heavy) compared to HEKNNMT cells (Light). (F) Cellular component analysis of the 235 enriched proteins. All experiments were performed in triplicate (n = 3).